

Multi-state Epidemic Processes on Complex Networks

Naoki Masuda*

*Laboratory for Mathematical Neuroscience, RIKEN Brain Science Institute, 2-1,
Hirosawa, Wako, Saitama 351-0198, Japan*

Norio Konno

*Faculty of Engineering, Yokohama National University, 79-5, Tokiwadai,
Hodogaya, Yokohama 240-8501, Japan*

Abstract

Realistic dynamics of infectious diseases are described by multi-state models with appropriate transition rules representing, for example, birth, death, infection, recovery, disease progression, and quarantine. We analyze various multi-state epidemic models on complex networks, or in ensembles of individuals with heterogeneous contact rates. In most models, as in the SIS model, heterogeneous degree distributions principally decrease the critical infection rates. In models with competing pathogens and mutation, however, further conditions must be satisfied for the heterogeneity effect to appear. Furthermore, the rock-scissors-paper game does not show this dependence. Our systematic approach enables us to predict effects of complex networks on general epidemic models.

Key words: epidemiology, complex networks, scale-free networks, contact process, critical infection rates

PACS: 89.75.Hc, 87.19.Xx, 87.23.Ge, 89.75.Da

* Corresponding author. Address: Laboratory for Mathematical Neuroscience, RIKEN Brain Science Institute, 2-1, Hirosawa, Wako, Saitama 351-0198, Japan, Phone:+81-48-467-9664, FAX:+81-48-467-9693
Email addresses: `masuda@brain.riken.jp` (Naoki Masuda),
`norio@mathlab.sci.ynu.ac.jp` (Norio Konno).

1 Introduction

Since late 1990s, real networks have been recognized to be complex and not approximated by conventional graphs such as lattices, regular trees, or classical random graphs. Not only being complex, many networks have the small-world and scale-free properties (Albert and Barabási, 2002; Newman, 2003). An important property of the small-world network is that the distance between a pair of vertices, or the minimum number of edges connecting two vertices, is fairly small on average. Also, the vertex degree k , or the number of edges for a vertex, is often distributed according to a scale-free distribution: $p_k \propto k^{-\gamma}$ (Barabási and Albert, 1999). Typically, γ ranges between 2 and 3 (Albert and Barabási, 2002; Newman, 2003).

Real data support that scale-free networks underly propagation of sexually transmitted diseases (Anderson and May, 1991; Colgate et al., 1989; Liljeros et al., 2001; Schneeberger et al., 2004) and computer viruses (Newman, 2003; Pastor-Satorras and Vespignani, 2001a). In line with this, theoretical studies with interacting particle systems have shown that the critical infection rates above which epidemic outbreaks or endemic states ensue scale as $\langle k \rangle / \langle k^2 \rangle$. This holds for the percolation (Albert et al., 2000; Cohen et al., 2000; Newman, 2002), the contact process (also called the SIS model) that describes endemic diseases (Pastor-Satorras and Vespignani, 2001a; Pastor-Satorras and Vespignani, 2001b), and the SIR models that describe single-shot outbreak dynamics (May and Lloyd, 2001; Moreno et al., 2002). Other related studies with spatial heterogeneity (Anderson and May, 1991, p.141) and the random walk (Masuda and Konno, 2004) are also supportive of this scenario. Scale-free networks with $\gamma \leq 3$ have epidemic thresholds equal to 0 because $\langle k^2 \rangle$

diverges.

Realistic epidemic processes are complex both in terms of networks and interactions. Particularly, multi-state models in which each vertex changes its state at properly designed rates of, for example, birth, death, infection, recovery, and mutation (Anderson and May, 1991; Andjel and Schinazi, 1996; Durrett and Neuhauser, 1991; Frean and Abraham, 2001; Haraguchi and Sasaki, 2000; Hopbauer and Sigmund, 1998; Joo and Lebowitz, 2004; Kobayashi et al., 2001; Krone, 1999; Konno et al., 2004; Liggett, 1985; Marro and Dickman, 1999; Sato et al., 1994; Sato and Konno, 1995; Sato et al., 1997; Schinazi, 1997; Schinazi, 1999; Schinazi, 2000; Schinazi, 2001a; Schinazi, 2001b; Schinazi, 2002; Schinazi, 2003; Szabó and Sznajder, 2004; Tainaka, 1994; Tainaka, 2003; van den Berg et al., 1998) may serve to understand relevance of complex networks to real epidemics. In this direction, there are just a few analyses. Liu and coworkers performed complex-network analysis of the SIRS model and the so-called household model to show the $\langle k \rangle / \langle k^2 \rangle$ -dependence of the critical infection rates (Liu et al., 2004a; Liu et al., 2004b).

In this paper, we perform complex network analysis of various multi-state epidemic processes originally proposed for lattices, trees, or meanfield interaction. The critical infection rates become extinct as $\langle k^2 \rangle \rightarrow \infty$, but with a couple of important exceptions described below. In Sec. 2, we review earlier results of the epidemic models on complex networks. Sections 3, 4, 5, 6, and 7 are devoted to analysis of the representative models classified according to transition rules. Short discussion follows in Sec. 8.

2 A Short Review of Basic Epidemic Processes

2.1 Contact Process

Let us start with the contact process on complex networks, or in heterogeneous populations (Anderson and May, 1991, Chapters 10, 11, 19); (Pastor-Satorras and Vespignani, 2001a; Pastor-Satorras and Vespignani, 2001b). The contact process is a continuous-time Markov process on a network in which an agent on each vertex takes either state 0 (susceptible) or state 1 (infected). As schematically shown in Fig. 1, a susceptible vertex is infected at a rate proportional to the infection rate λ and the number of infected vertices in its neighborhood. An infected vertex spontaneously becomes healed after a random time, whose mean is set 1 without losing generality. The cured individual is not assumed to acquire immunity. On lattices and regular trees, there are nontrivial critical infection rates, denoted by λ_c , only above which vertices of state 1 persist in infinite time with a positive probability (Liggett, 1985, Ch. 6); (Marro and Dickman, 1999, Ch. 6). This situation corresponds to the endemic state in which the states 0 and 1 can coexist.

Let us denote by p_k the probability that a vertex has degree k . Obviously, $\sum_{k=1}^{\infty} p_k = 1$, and the mean degree $\langle k \rangle \equiv \sum_{k=1}^{\infty} k p_k$. We denote by $\rho_{1,k}$ the number of vertices with degree k and state 1 divided by all the vertices with degree k . The portion of vertices with state 0 among those with degree k is equal to $1 - \rho_{1,k}$. The meanfield dynamics are

$$\dot{\rho}_{1,k} = \lambda k (1 - \rho_{1,k}) \Theta_1 - \rho_{1,k}, \quad (k = 1, 2, \dots) \quad (1)$$

where the first and second terms of Eq. (1) represent the mean transition rates

from 0 to 1 and from 1 to 0, respectively. The probability that a neighborhood located on the end of a randomly chosen edge takes state 1, denoted by Θ_1 , becomes

$$\Theta_1 = \frac{\sum_k k p_k \rho_{1,k}(t)}{\langle k \rangle}. \quad (2)$$

In the equilibrium, we obtain

$$\rho_{1,k}^* = \frac{\lambda k \Theta_1^*}{1 + \lambda k \Theta_1^*}, \quad (3)$$

where $*$ indicate the steady state. Plugging Eq. (3) into Eq. (2) leads to

$$\Theta_1^* = \frac{1}{\langle k \rangle} \sum_k \frac{\lambda \Theta_1^* k^2 p_k}{1 + \lambda \Theta_1^* k}. \quad (4)$$

Equation (4) holds when $\Theta^* = 0$, corresponding to the disease-free state denoted by $\{0\}$. When $0 < \Theta^* < 1$, two states coexist ($\{0, 1\}$). Since the RHS of Eq. (4) is equal to (smaller than) the LHS when $\Theta^* = 0$ ($\Theta^* = 1$),

$$\left. \frac{\partial}{\partial \Theta_1^*} \left(\frac{1}{\langle k \rangle} \sum_k \frac{\lambda \Theta_1^* k^2 p_k}{1 + \lambda \Theta_1^* k} \right) \right|_{\Theta_1^*=0} > 1 \quad (5)$$

is a sufficient condition for the $\{0, 1\}$ phase. Equations (5) guarantees that

$$\lambda_c = \frac{\langle k \rangle}{\langle k^2 \rangle} \quad (6)$$

divides $\{0\}$ and $\{0, 1\}$. When $p_k \propto k^{-\gamma}$ ($\gamma \leq 3$), we have $\lambda_c = 0$.

2.2 SIRS-type Models

Figure 2 is the transition rule of a variant of the SIRS model. The states 0, 1, and 2 respectively represent susceptible, infected, and recovered. After recov-

ery at rate μ , immunity persists for a random time with mean 1 before coming back to the susceptible state. The state 2 can be also considered as empty, if the birth process ($2 \rightarrow 0$) is roughly independent of the neighbors' states, as for forest trees. This model extends the contact process, which corresponds to $\mu = 0$ and $\delta = 1$.

The meanfield analysis predicts that two phases $\{0\}$ and $\{0, 1, 2\}$ are separated by $\lambda = \mu + \delta$. On regular lattices, the critical infection rate λ_c rigorously exists for $\delta = 0$ and $\mu > 0$ (Andjel and Schinazi, 1996; Durrett and Neuhauser, 1991; van den Berg et al., 1998), and λ quantitatively influences the survival probability more than μ does (Joo and Lebowitz, 2004; Kobayashi et al., 2001).

With heterogeneous contact rates, λ_c behaves essentially in the same manner as Eq. (6) (Liu et al., 2004a). Let us briefly review the analysis; denote the proportion of vertices with state i ($i = 0, 1, 2$) and degree k by $\rho_{i,k}$. Noting that $\rho_{0,k} + \rho_{1,k} + \rho_{2,k} = 1$, the meanfield dynamics are given by

$$\begin{aligned}\dot{\rho}_{1,k} &= \lambda(1 - \rho_{1,k} - \rho_{2,k})k\Theta_1 - (\mu + \delta)\rho_{1,k}, \\ \dot{\rho}_{2,k} &= \mu\rho_{1,k} - \rho_{2,k},\end{aligned}\tag{7}$$

whose steady state is

$$\rho_{1,k}^* = \frac{\rho_{2,k}^*}{\mu} = \frac{\lambda k \Theta_1^*}{\mu + \delta + \lambda(\mu + 1)\Theta_1^* k}.\tag{8}$$

The $\{0, 1, 2\}$ phase requires $\Theta_1^* > 0$. With Eqs. (2) and (8), we derive

$$\Theta_1^* = \frac{1}{\langle k \rangle} \sum_k \frac{\lambda \Theta_1^* k^2 p_k}{\mu + \delta + \lambda(\mu + 1)\Theta_1^* k},\tag{9}$$

and

$$\lambda_c = (\mu + \delta) \langle k \rangle / \langle k^2 \rangle.\tag{10}$$

The result has also been extended (Liu et al., 2004b) to another variant called the household model (Schinazi, 2002).

3 Models with Single Neighbor-dependent Transition

In the following sections, we investigate various contagion models with different transition rules. Since we can never be exhaustive, our strategy is to study known models. The essential factor turns out to be the gross organization of the transition pathways independent of the state of the neighbors (solid lines in Figs. 1 and 2) and those dependent on the density of neighbors in certain states (dashed lines). We begin with some models that have just one neighbor-dependent transition rule.

3.1 Two-stage Contact Process

Two-stage contact process whose rule is shown in Fig. 3(A) (Krone, 1999) differs from the SIRS model (Fig. 2) in that the transition rate from 0 to 1 is proportional to the density of the neighbors with state 2 (not 1) of a state-0 vertex. The states can be interpreted as 0: vacant, 1: occupied by young individuals, 2: occupied by adults, or 0: vacant, 1: partially occupied, 2: fully occupied colonies, with only adults or fully occupied colonies capable of generating offsprings. The ordinary contact process is reproduced as $\mu = \infty$. The meanfield approximation and the rigorous results on regular lattices conclude that $\{0\}$ and $\{0, 1, 2\}$ exist. Naturally, large λ or μ promotes survival (Krone, 1999).

The meanfield dynamics on complex networks are given by

$$\begin{aligned}\dot{\rho}_{1,k} &= \lambda(1 - \rho_{1,k} - \rho_{2,k})k\Theta_2 - (\delta + r)\rho_{1,k}, \\ \dot{\rho}_{2,k} &= r\rho_{1,k} - \rho_{2,k},\end{aligned}\tag{11}$$

where Θ_2 is determined analogously to Eq. (2). The steady state is

$$\begin{aligned}\rho_{1,k}^* &= \frac{\rho_{2,k}^*}{r}, \\ \rho_{2,k}^* &= \frac{\lambda r \Theta_2^* k}{\delta + r + \lambda(r+1)\Theta_2^* k},\end{aligned}\tag{12}$$

which guarantees that

$$\Theta_2^* = \frac{1}{\langle k \rangle} \sum_k \frac{\lambda r \Theta_2^* k^2 p_k}{\delta + r + \lambda(r+1)\Theta_2^* k} > 0\tag{13}$$

is necessary and sufficient for the $\{0, 1, 2\}$ phase. The phase $\{0, 1, 2\}$ appears when the RHS of Eq. (13) is larger than the LHS as $\Theta_2^* \rightarrow 0$, which yields

$$\lambda > \frac{(\delta + r) \langle k \rangle}{r \langle k^2 \rangle}.\tag{14}$$

3.2 Tuberculosis Model

A next example is a tuberculosis model shown in Fig. 3(B) (Schinazi, 2003). In the tuberculosis, a majority of the infected does not become infectious. Accordingly, we can interpret 0: healthy, 1: infected but not infectious, and 2: infected and infectious. Although this model is an obvious extension of the two-stage contact process, which corresponds to $\mu = 0$, it has two important features. One is that we have two pathways of neighbor-dependent transmission rates, both of which depend on the density of state 2. The other is that disease progression from state 1 to 2 is possible through two parallel routes. When $r = 0$, the $\{0, 1, 2\}$ phase is impossible in perfectly mixed populations and possible on regular lattices (Schinazi, 2003).

In heterogeneous populations, the dynamics become

$$\begin{aligned}\dot{\rho}_{1,k} &= \lambda(1 - \rho_{1,k} - \rho_{2,k})k\Theta_2 - \mu\rho_{1,k}k\Theta_2 - (\delta + r)\rho_{1,k}, \\ \dot{\rho}_{2,k} &= \mu\rho_{1,k}k\Theta_2 + r\rho_{1,k} - \rho_{2,k}.\end{aligned}\tag{15}$$

The steady state is given by

$$\begin{pmatrix} \rho_{1,k}^* \\ \rho_{2,k}^* \end{pmatrix} = \frac{\lambda\Theta_2^*k}{\delta + r + (\lambda + \mu + \lambda r)\Theta_2^*k + \lambda\mu\Theta_2^{*2}k^2} \begin{pmatrix} 1 \\ r + \mu k\Theta_2^* \end{pmatrix},\tag{16}$$

and

$$\Theta_2^* = \frac{1}{\langle k \rangle} \sum_k \frac{\lambda k^2 (r + \mu k\Theta_2^*)\Theta_2^* p_k}{\delta + r + (\lambda + \mu + \lambda r)k\Theta_2^* + \lambda\mu k^2\Theta_2^{*2}}.\tag{17}$$

The $\{0, 1, 2\}$ phase appears when $\Theta_2^* > 0$, or

$$\lambda > \frac{(\delta + r)\langle k \rangle}{r\langle k^2 \rangle}.\tag{18}$$

4 Models with Competing Pathogens

In many situations, susceptible individuals are subject to multiple strains of pathogens that often compete with each other. In terms of schematic diagrams like Figs. 1, 2, and 3, this means that multiple types of neighbor-dependent infection pathways (dashed lines) emanate from one state. On top of that, transitions between the infectious states can occur because of mutation or disease progression.

4.1 Example 1

In the example 1 shown in Fig. 4(A), state 1 and state 2 compete to devour state 0 at rates β_1 and β_2 , respectively. Mutations only from 1 to 2 are allowed (Schinazi, 2001a). The three states can be interpreted as 0: empty, 1: species A, 2: species B, or 0: susceptible, 1: patients with strain A, 2: patients with strain B.

Exploiting the fact that the absence of state-1 vertices means the contact process, Schinazi showed for regular lattices that there are three phases $\{0\}$, $\{0, 2\}$, and $\{0, 1, 2\}$ divided by nontrivial critical lines (Schinazi, 2001a). Small r and large β_1 reinforces the $\{0, 1, 2\}$ state. Based on the meanfield analysis, the boundary between $\{0\}$ and $\{0, 2\}$ is $\beta_2 = 1$, and the boundary between $\{0, 2\}$ and $\{0, 1, 2\}$ is $\beta_1 = \beta_2(r + 1)$.

For heterogeneous populations, the dynamics are given by

$$\begin{aligned}\dot{\rho}_{1,k} &= \beta_1 (1 - \rho_{1,k} - \rho_{2,k}) k \Theta_1 - (r + 1) \rho_{1,k}, \\ \dot{\rho}_{2,k} &= \beta_2 (1 - \rho_{1,k} - \rho_{2,k}) k \Theta_2 + r \rho_{1,k} - \rho_{2,k}.\end{aligned}\tag{19}$$

The results in Sec. 2.1 implies that $\{0, 2\}$ emerges when

$$\beta_2 > \frac{\langle k \rangle}{\langle k^2 \rangle}.\tag{20}$$

With the steady state

$$\begin{pmatrix} \rho_{1,k}^* \\ \rho_{2,k}^* \end{pmatrix} = \frac{k}{r + 1 + (r + 1) (\beta_2 \Theta_2^* + \beta_1 \Theta_1^*) k} \begin{pmatrix} \beta_1 \Theta_1^* \\ \beta_1 r \Theta_1^* + \beta_2 (r + 1) \Theta_2^* \end{pmatrix},\tag{21}$$

we obtain

$$\Theta_1^* = \frac{\beta_1 - \beta_2(r+1)}{r\beta_1} \Theta_2^* \equiv C\Theta_2^*, \quad (22)$$

and

$$\Theta_2^* = \frac{1}{\langle k \rangle (r+1)} \sum_k \frac{\beta_1 \Theta_2^* k^2 p_k}{1 + (\beta_1 C + \beta_2) \Theta_2^* k}. \quad (23)$$

The first condition for the $\{0, 1, 2\}$ phase is $\Theta_2^* > 0$, which results in

$$\beta_1 > \frac{(r+1) \langle k \rangle}{\langle k^2 \rangle}. \quad (24)$$

The second is $\beta_1 > \beta_2(r+1)$, which comes from $\Theta_1^* > 0$. This condition coincides with that obtained by the meanfield analysis and is independent of degree distributions.

Figure 5 shows numerically obtained steady densities of state 1 (A) and 2 (B) in networks with 10000 vertices and $\langle k \rangle = 12$. We set $\beta_1 = 0.5$ and $\beta_2 = 0.25$, and the initial conditions are such that each vertex takes one of the three states independently with probability $1/3$. The scale-free networks with the scaling exponent $\gamma = 2.5$ (thickest solid lines), $\gamma = 3.0$ (moderate solid lines), and $\gamma = 4.0$ (thinnest solid lines) are produced using a static scale-free network model (Goh et al., 2001). Even though produced networks can be disconnected in general, more than 95 % of the vertices constitute one component in every run of our simulations. The results for the random graph, which correspond to the meanfield situation, are also shown (dashed lines). Regardless of the network type, the numerical results support the existence of finite thresholds of r slightly smaller than the meanfield prediction $r = \beta_1/\beta_2 - 1 = 1$.

4.2 Example 2

A four-state model shown in Fig. 4(B) accounts for spread of a drug-resistant strain, which may be caused by misuse of antibiotics (Schinazi, 1999). The states 0, 1, 2, and 3 represent empty, susceptible, infected with the wild strain, and infected with the drug-resistant strain, respectively. The states 2 and 3 compete with each other, and ϕ is the mutation rate. The model without state 2 (or $\beta_2 = 0$) is equivalent to the SIRS model in Fig. 2 with $\delta = 0$. On lattices, $\{0, 1, 2, 3\}$ appears when $r + \phi$ is small enough. Otherwise, state 2 is extinguished (Schinazi, 1999). Based on the meanfield analysis, the $\{0, 1, 2, 3\}$ phase ensues when

$$\phi > 0, \quad \beta_2 > r + \phi, \quad \frac{\beta_2}{r + \phi} > \beta_3. \quad (25)$$

If any of the conditions in Eq. (25) is violated and $\beta_3 > 1$, then we have $\{0, 1, 3\}$. Otherwise, only $\{1\}$ is viable.

On complex networks, starting with

$$\begin{aligned} \dot{\rho}_{1,k} &= \beta_1 (1 - \rho_{1,k} - \rho_{2,k} - \rho_{3,k}) + r\rho_{2,k} - \beta_2\rho_{1,k}k\Theta_2 - \beta_3\rho_{1,k}k\Theta_3, \\ \dot{\rho}_{2,k} &= \beta_2\rho_{1,k}k\Theta_2 - (r + \phi)\rho_{2,k}, \\ \dot{\rho}_{3,k} &= \beta_3\rho_{1,k}k\Theta_3 + \phi\rho_{2,k} - \rho_{3,k}, \end{aligned} \quad (26)$$

we obtain

$$\begin{pmatrix} \rho_{1,k}^* \\ \rho_{2,k}^* \\ \rho_{3,k}^* \end{pmatrix} = \frac{\beta_1}{\Delta} \begin{pmatrix} r + \phi \\ \beta_2\Theta_2^*k \\ [\beta_2\phi\Theta_2^* + \beta_3(r + \phi)\Theta_3^*]k \end{pmatrix}, \quad (27)$$

where

$$\Delta \equiv \beta_1(r + \phi) + [(\beta_1 + \phi + \beta_1\phi) \beta_2 \Theta_2^* + (\beta_1 + 1) \beta_3 (r + \phi) \Theta_3^*] k. \quad (28)$$

Equation (27) assures that $\rho_{1,k}^* > 0$. In addition,

$$\Theta_3^* = \frac{\beta_2 \phi}{\beta_2 - \beta_3(r + \phi)} \Theta_2^* \equiv C \Theta_2^* \quad (29)$$

provided that $\beta_2/(r + \phi) > \beta_3$. Under this condition, $\Theta_2^* > 0$ is equivalent to the $\{0, 1, 2, 3\}$ phase. Combining the definition of Θ_2^* analogous to Eq. (2) with Eqs. (27) and (29) results in

$$\Theta_2^* = \frac{1}{\langle k \rangle} \sum_k \frac{\beta_2 \Theta_2^* k^2 p_k}{\Delta}. \quad (30)$$

Since Δ is of the form: $\Delta = c_1 + c_2 k \Theta_2^*$, Eq. (30) is essentially the same as Eq. (4). Accordingly, $\{0, 1, 2, 3\}$ appears when

$$\beta_2 > \frac{\beta_1(r + \phi) \langle k \rangle}{\langle k^2 \rangle}. \quad (31)$$

Even for large $r + \phi$, sufficiently heterogeneous p_k with large $\langle k^2 \rangle / \langle k \rangle$ allows eventual existence of state 2. For this to occur, the last of the three conditions in Eq. (25), which is independent of degree distributions, is needed.

If $\beta_2/(r + \phi) \leq \beta_3$, then $\Theta_2^* = 0$, and Eq. (27) reduces to

$$\begin{pmatrix} \rho_{1,k}^* \\ \rho_{3,k}^* \end{pmatrix} = \frac{\beta_1}{\beta_1 + (\beta_1 + 1) \beta_3 \Theta_3^* k} \begin{pmatrix} 1 \\ \beta_3 \Theta_3^* k \end{pmatrix}, \quad (32)$$

which yields

$$\Theta_3^* = \frac{1}{\langle k \rangle} \sum_k \frac{\beta_1 \beta_3 \Theta_3^* k^2 p_k}{\beta_1 + (\beta_1 + 1) \beta_3 \Theta_3^* k}. \quad (33)$$

As a result, $\{0, 1, 3\}$ and $\{1\}$ is separated by

$$\beta_3 = \frac{\langle k \rangle}{\langle k^2 \rangle}. \quad (34)$$

Both $\{1\}$ and $\{0, 1, 3\}$ disappear when $\langle k^2 \rangle = \infty$ and $\beta_2/(r + \phi) > \beta_3$. In this situation, the $\{0, 1, 2, 3\}$ phase dominates even for infinitesimally small infection rates.

4.3 Example 3

Superspreaders, namely, patients that infect many others in comparison with normal patients, are identified in the outbreaks in HIV/AIDS (Colgate et al., 1989), SARS, (Abdullah et al., 2003; Leo et al., 2003), and gonorrhea (Anderson and May, 1991, p. 230). Such heterogeneous infection rates are partially ascribed to heterogeneous social or sexual contact rates as specified by p_k . However, superspreaders exist even in diseases whose associated networks are considered to have relatively homogeneous k , such as SARS (Masuda et al., 2004).

Accordingly, we analyze a three-state model with different infection rates schematically shown in Fig. 4(C) (Schinazi, 2001b). The states 0, 1, and 2 mean susceptible, patients of type 1 with infection rate λ_1 and recovery rate 1, and patients of type 2 with infection rate $\lambda_1 \geq \lambda_2$ and recovery rate δ , respectively. State 2 corresponds to the superspreader. Upon infection, a state-0

vertex changes its state into 1 (2) with probability $1 - p$ (p). There are two neighbor-dependent infection routes in Fig. 4(C), and they indirectly compete with each other through crosstalk, which means that the density of state 1 and that of state 2 affect the transitions $0 \rightarrow 2$ and $0 \rightarrow 1$, respectively. The meanfield analysis indicates that $\{0, 1, 2\}$ results when

$$\lambda_1 \delta (1 - p) + \lambda_2 p > \delta. \quad (35)$$

Otherwise, $\{0\}$ results. Slightly weaker but qualitatively similar results have been proved for lattices (Schinazi, 2001b).

In heterogeneous populations, dynamics are given by

$$\begin{aligned} \dot{\rho}_{1,k} &= (1 - p) (1 - \rho_{1,k} - \rho_{2,k}) k (\lambda_1 \Theta_1 + \lambda_2 \Theta_2) - \rho_{1,k}, \\ \dot{\rho}_{2,k} &= p (1 - \rho_{1,k} - \rho_{2,k}) k (\lambda_1 \Theta_1 + \lambda_2 \Theta_2) - \delta \rho_{2,k}. \end{aligned} \quad (36)$$

The steady state is:

$$\begin{pmatrix} \rho_{1,k}^* \\ \rho_{2,k}^* \end{pmatrix} = \frac{(\lambda_1 \Theta_1^* + \lambda_2 \Theta_2^*) k}{\delta + [p + \delta (1 - p)] (\lambda_1 \Theta_1^* + \lambda_2 \Theta_2^*) k} \begin{pmatrix} \delta (1 - p) \\ p \end{pmatrix}, \quad (37)$$

which leads to

$$\Theta_1^* = \frac{\delta (1 - p)}{p} \Theta_2^*. \quad (38)$$

Therefore, $\Theta_1^* > 0$, or equivalently, $\bar{\Theta}^* \equiv \lambda_1 \Theta_1^* + \lambda_2 \Theta_2^* > 0$, is the condition for the $\{0, 1, 2\}$ phase. With Eq. (37), we obtain

$$\bar{\Theta}^* = \frac{1}{\langle k \rangle} \sum_k \frac{[\lambda_1 \delta (1 - p) + \lambda_2 p] \bar{\Theta}^* k^2 p_k}{\delta + [p + \delta (1 - p)] k \bar{\Theta}^*}, \quad (39)$$

and $\{0, 1, 2\}$ emerges when

$$\lambda_1 \delta (1 - p) + \lambda_2 p > \frac{\delta \langle k \rangle}{\langle k^2 \rangle}. \quad (40)$$

Equation (40) suggests that an arbitrary small infection rate λ_1 or λ_2 allows the endemic state.

5 Essentially Two Types of Neighbor-dependent Transitions

We deal with the model shown in Fig. 6, in which state 0, 1, and 2 mean empty, susceptible, and infected, respectively. In this model, a susceptible gives birth to an offspring on an empty vertex. An alternative interpretation is 0: susceptible, 1: infected, and 2: infected by another pathogen. In this case, state 2 may more virulent than state 1 (Haraguchi and Sasaki, 2000; Sato et al., 1994), and state 2 feeds not on state 0 but on state 1. The model extends the contact process and the SIR model, which correspond to $\mu = r = 0$ and $\lambda = \delta = 0$, respectively.

This model is most intricate of all examined in this paper. This subtlety stems from the consecutive neighbor-dependent transitions from 0 to 1 and from 1 to 2 (also see discussion in (Andjel and Schinazi, 1996; Durrett and Neuhauser, 1991)). Neighbor-dependent transitions are cascaded in some other contagion models as well (Sato and Konno, 1995; Schinazi, 1997; Schinazi, 2000; Tainaka, 2003).

The model gives rise to paradoxical behavior on lattices; for example, an increase in λ lessens state-1 vertices because a larger λ creates more preys to devour for state-2 vertices (Tainaka, 2003). Similarly, too large μ drives state

2 to perish due to excess mortality (Haraguchi and Sasaki, 2000; Sato et al., 1994), which defines a phase qualitatively different from $\{0\}$, $\{0, 1\}$, and $\{0, 1, 2\}$ revealed by analytical calculations (Haraguchi and Sasaki, 2000; Sato et al., 1994; Tainaka, 2003; Konno et al., 2004).

Regarding the three basic phases, the one-dimensional lattice with $r = 0$ does not permit $\{0, 1, 2\}$ (Andjel and Schinazi, 1996; Sato et al., 1994). This also holds true for the two-dimensional lattice with sufficiently small r (Konno et al., 2004), although the meanfield theory predicts the $\{0, 1, 2\}$ phase for any $r > 0$. The phase diagram in the parameter space is even qualitatively unknown for lattices. For explanation, we set $r = 0$ and fix $\delta > 0$. The meanfield solution divides $\{0\}$ and $\{0, 1\}$ by $\lambda = \delta$, and $\{0, 1\}$ and $\{0, 1, 2\}$ by $\mu = \lambda/(\lambda - \delta)$. Accordingly, the two critical lines approach each other asymptotically in the λ - μ space. On the other hand, they may cross at finite λ and μ , as supported by the improved pair approximation ansatz (Haraguchi and Sasaki, 2000; Sato et al., 1994).

In heterogeneous populations, the dynamics read

$$\begin{aligned}\dot{\rho}_{1,k} &= \lambda(1 - \rho_{1,k} - \rho_{2,k})k\Theta_1 - (\delta + r)\rho_{1,k} - \mu\rho_{1,k}k\Theta_2, \\ \dot{\rho}_{2,k} &= \mu\rho_{1,k}k\Theta_2 + r\rho_{1,k} - \rho_{2,k}.\end{aligned}\tag{41}$$

The steady state is given by

$$\begin{pmatrix} \rho_{1,k}^* \\ \rho_{2,k}^* \end{pmatrix} = \frac{\lambda\Theta_1^*k}{\delta + r + [\lambda(r + 1)\Theta_1^* + \mu\Theta_2^*]k + \lambda\mu\Theta_1^*\Theta_2^*k^2} \begin{pmatrix} 1 \\ \mu\Theta_2^*k + r \end{pmatrix}, \tag{42}$$

which leads to

$$\begin{pmatrix} \Theta_1^* \\ \Theta_2^* \end{pmatrix} = \frac{1}{\langle k \rangle} \sum_k \frac{\lambda \Theta_1^*}{\delta + r + [\lambda(r+1)\Theta_1^* + \mu\Theta_2^*]k + \lambda\mu\Theta_1^*\Theta_2^*k^2} \begin{pmatrix} k^2 p_k \\ (\mu\Theta_2^*k + r)k^2 p_k \end{pmatrix}. \quad (43)$$

Clearly, $(\Theta_1^*, \Theta_2^*) = (0, 0)$, which corresponds to the $\{0\}$ phase, solves Eq. (43).

To explore other phases, let us set

$$f_1(\Theta_1^*, \Theta_2^*) \equiv \frac{\lambda}{\langle k \rangle} \sum_k \frac{k^2 p_k}{\delta + r + [\lambda(r+1)\Theta_1^* + \mu\Theta_2^*]k + \lambda\mu\Theta_1^*\Theta_2^*k^2} - 1, \quad (44)$$

and

$$f_2(\Theta_1^*, \Theta_2^*) \equiv \frac{\lambda\Theta_1^*}{\langle k \rangle} \sum_k \frac{(\mu\Theta_2^*k + r)k^2 p_k}{\delta + r + [\lambda(r+1)\Theta_1^* + \mu\Theta_2^*]k + \lambda\mu\Theta_1^*\Theta_2^*k^2} - \Theta_2^*. \quad (45)$$

Then Eq. (43) is equivalent to $\Theta_1^* f_1(\Theta_1^*, \Theta_2^*) = 0$ and $f_2(\Theta_1^*, \Theta_2^*) = 0$. The functions f_1 and f_2 have the following properties:

$$f_1(0, 0) = \frac{\lambda \langle k^2 \rangle}{(\delta + r) \langle k \rangle} - 1, \quad (46)$$

$$\begin{aligned} f_1(1, 0) &= \frac{\lambda}{\langle k \rangle} \sum_k \frac{k^2 p_k}{\delta + r + \lambda(r+1)k} - 1 \\ &\leq \frac{\lambda}{\langle k \rangle} \sum_k \frac{k^2 p_k}{\lambda(r+1)k} - 1 \leq 0, \end{aligned} \quad (47)$$

$$f_1(0, 1) = \frac{\lambda}{\langle k \rangle} \sum_k \frac{k^2 p_k}{\delta + r + \mu k} - 1, \quad (48)$$

$$\frac{\partial f_1}{\partial \Theta_1^*} < 0, \quad (49)$$

$$\frac{\partial f_1}{\partial \Theta_2^*} < 0, \quad (50)$$

$$\frac{\partial f_2}{\partial \Theta_1^*} > 0, \quad (51)$$

$$\frac{\partial f_2(0, \Theta_2^*)}{\partial \Theta_2^*} = -1. \quad (52)$$

To examine the $\{0, 1\}$ phase, we set $\Theta_2^* = 0$ and look for $0 < \Theta_1^* < 1$ that satisfies $f_1(\Theta_1^*, 0) = 0$ and $f_2(\Theta_1^*, 0) = 0$ simultaneously. These conditions in combination with Eq. (45) yield $r = 0$. By substituting $r = 0$ and $\Theta_2^* = 0$ into Eq. (44), we obtain

$$f_1(\Theta_1^*, 0) = \frac{\lambda}{\langle k \rangle} \sum_k \frac{k^2 p_k}{\delta + \lambda \Theta_1^* k} - 1 = 0. \quad (53)$$

Based on Eq. (47), Eq. (53) is satisfied when $f_1(0, 0) > 0$, that is,

$$\lambda > \frac{\delta \langle k \rangle}{\langle k^2 \rangle}. \quad (54)$$

It is easy to verify that Eq. (54) is valid both for $\delta > 0$ and $\delta = 0$. This conclusion is naturally consistent with that of the contact process (see Sec. 2.1).

The potential $\{0, 1, 2\}$ phase should accommodate $\Theta_1^* > 0$ and $\Theta_2^* > 0$ so that $f_1(\Theta_1^*, \Theta_2^*) = 0$ and $f_2(\Theta_1^*, \Theta_2^*) = 0$. Since we are primarily concerned to the case in which $\langle k^2 \rangle$ is large, let us assume that $f_1(0, 0)$ given in Eq. (46) is positive. This is just a trivial extension of Eq. (54) to general $r \geq 0$. Then, Eqs. (47), (49), and the continuity of f_1 in Θ_1^* and Θ_2^* guarantee that there is a unique $0 < \bar{\Theta}_1 \leq 1$ such that $f_1(\bar{\Theta}_1, 0) = 0$. Based on Eqs. (49) and (50), there is a curve $f_1(\Theta_1^*, \Theta_2^*) = 0$ in the Θ_1^* - Θ_2^* space that looks like (I) (when $f_1(0, 1) \leq 0$), or (II) (when $f_1(0, 1) > 0$) in Fig. 7(A).

When $r > 0$, with Eqs. (51), (52), and $f_2(0, 0) = 0$, we obtain $f_2(1, 0) > 0$ and $f_2(0, 1) < 0$. Then, from the continuity of f_2 in Θ_1^* and Θ_2^* , there is a $0 < \bar{\Theta} < 1$ so that $f_2(\bar{\Theta}, 1 - \bar{\Theta}) = 0$. If $f_1(\bar{\Theta}, 1 - \bar{\Theta}) < 0$, a curve $f_2(\Theta_1^*, \Theta_2^*) = 0$ is like the dashed line in Fig. 7(B) and crosses $f_1(\Theta_1^*, \Theta_2^*) = 0$ (one of the solid lines). Then we obtain the $\{0, 1, 2\}$ phase. Let us note that our argument does not require uniqueness of the curves. The condition $f_1(\bar{\Theta}, 1 - \bar{\Theta}) < 0$ is actually

satisfied since, with

$$C_1 \equiv \frac{\lambda}{\lambda(r+1)\bar{\Theta} + \mu(1-\bar{\Theta}) - \lambda r \bar{\Theta}}, \quad (55)$$

we derive

$$\begin{aligned} & f_1(\bar{\Theta}, 1 - \bar{\Theta}) \\ &= f_1(\bar{\Theta}, 1 - \bar{\Theta}) + C_1 f_2(\bar{\Theta}, 1 - \bar{\Theta}) \\ &= \frac{\lambda}{\langle k \rangle} \sum_k \frac{k^2 p_k + C_1 \bar{\Theta} (\mu k (1 - \bar{\Theta}) + r) k^2 p_k}{\delta + r + [\lambda(r+1)\bar{\Theta} + \mu(1-\bar{\Theta})] k + \lambda \mu \bar{\Theta} (1 - \bar{\Theta}) k^2} - 1 - C_1(1 - \bar{\Theta}) \\ &< \frac{\lambda}{\langle k \rangle} \sum_k \frac{k^2 p_k + C_1 \bar{\Theta} (\mu k (1 - \bar{\Theta}) + r) k^2 p_k}{[\lambda(r+1)\bar{\Theta} + \mu(1-\bar{\Theta})] k + \lambda \mu \bar{\Theta} (1 - \bar{\Theta}) k^2} - 1 - C_1(1 - \bar{\Theta}) \\ &= -\frac{\mu(1-\bar{\Theta})}{\lambda \bar{\Theta} + \mu(1-\bar{\Theta})} \leq 0. \end{aligned} \quad (56)$$

When $r = 0$, it is convenient to divide Eq. (45) by $\Theta_2^* > 0$ to redefine f_2 .

Equation (45) reduces to

$$f_2(\Theta_1^*, \Theta_2^*) \equiv \frac{\lambda \Theta_1^*}{\langle k \rangle} \sum_k \frac{\mu k^3 p_k}{\delta + [\lambda \Theta_1^* + \mu \Theta_2^*] k + \lambda \mu \Theta_1^* \Theta_2^* k^2} - 1. \quad (57)$$

Noting $f_2(0, \Theta_2^*) = -1$ ($0 \leq \Theta_2^* \leq 1$) and Eq. (51), $f_2(\Theta_1^*, \Theta_2^*) = 0$ must be like the dashed line in Fig. 7(C) so that it nontrivially crosses $f_1(\Theta_1^*, \Theta_2^*) = 0$.

Then, we require (i) $f_2(\bar{\Theta}_1, 0) > 0$ and (ii) $f_1(\bar{\Theta}, 1 - \bar{\Theta}) < 0$. The condition (i) is satisfied for large $\langle k^2 \rangle$ because, using

$$f_1(\bar{\Theta}_1, 0) = \frac{\lambda}{\langle k \rangle} \sum_k \frac{k^2 p_k}{\delta + \lambda \bar{\Theta}_1 k} - 1 = 0, \quad (58)$$

we obtain

$$f_2(\bar{\Theta}_1, 0) = \frac{\lambda \bar{\Theta}_1}{\langle k \rangle} \sum_k \frac{\mu k^3 p_k}{\delta + \lambda \bar{\Theta}_1 k} - 1$$

$$\begin{aligned}
&= \frac{\lambda \bar{\Theta}_1}{\langle k \rangle} \sum_k \frac{\mu k^3 p_k}{\delta + \lambda \bar{\Theta}_1 k} - 1 + \frac{\mu \delta}{\lambda} f_1(\bar{\Theta}_1, 0) \\
&= \frac{\langle k^2 \rangle}{\langle k \rangle} \mu - \left(1 + \frac{\mu \delta}{\lambda} \right) > 0.
\end{aligned} \tag{59}$$

To show (ii), we proceed similarly to the derivation of Eq. (56). With

$$C_2 \equiv \frac{\lambda(1 - \bar{\Theta})}{\lambda \bar{\Theta} + \mu(1 - \bar{\Theta})}, \tag{60}$$

we obtain

$$\begin{aligned}
&f_1(\bar{\Theta}, 1 - \bar{\Theta}) \\
&= f_1(\bar{\Theta}, 1 - \bar{\Theta}) + C_2 f_2(\bar{\Theta}, 1 - \bar{\Theta}) \\
&= \frac{\lambda}{\langle k \rangle} \sum_k \frac{k^2 p_k + C_2 \lambda \mu \bar{\Theta} k^3 p_k}{\delta + [\lambda \bar{\Theta} + \mu(1 - \bar{\Theta})] k + \lambda \mu \bar{\Theta}(1 - \bar{\Theta}) k^2} - 1 - C_2 \\
&< \frac{\lambda}{\langle k \rangle} \sum_k \frac{k^2 p_k + C_2 \lambda \mu \bar{\Theta} k^3 p_k}{[\lambda \bar{\Theta} + \mu(1 - \bar{\Theta})] k + \lambda \mu \bar{\Theta}(1 - \bar{\Theta}) k^2} - 1 - C_2 \\
&= -\frac{\mu(1 - \bar{\Theta})}{\lambda \bar{\Theta} + \mu(1 - \bar{\Theta})} \leq 0.
\end{aligned} \tag{61}$$

To summarize, the $\{0\}$ and $\{0, 1\}$ phases disappear as $\langle k^2 \rangle \rightarrow \infty$.

6 Rock-Scissors-Paper Game

The Rock-Scissors-Paper game models a cyclic competition of three states in which there is no absolute winner (Fig. 8(A)). Without spatial structure, there is no phase transition, and the only phase is a neutrally stable periodic orbit in which the densities of states 0, 1, and 2 wax and wane alternatively and cyclically (Hopbauer and Sigmund, 1998). Convergence to $\{0, 1, 2\}$ is more preferred on regular lattices (Frean and Abraham, 2001; Tainaka, 1994); (Marro and Dickman, 1999, p. 299) and trees (Sato et al., 1997), although periodic behavior is also observed.

For tractability, we focus on the steady states only. The dynamics in heterogeneous populations are given by

$$\begin{aligned}\dot{\rho}_{1,k} &= \lambda(1 - \rho_{1,k} - \rho_{2,k})k\Theta_1 - \mu\rho_{1,k}k\Theta_2, \\ \dot{\rho}_{2,k} &= \mu\rho_{1,k}k\Theta_2 - \rho_{2,k}k(1 - \Theta_1 - \Theta_2),\end{aligned}\tag{62}$$

which yields

$$\begin{pmatrix} \rho_{1,k}^* \\ \rho_{2,k}^* \end{pmatrix} = \frac{\lambda\Theta_1^*}{(\lambda\Theta_1^* + \mu\Theta_2^*)(1 - \Theta_1^* - \Theta_2^*) + \lambda\mu\Theta_1^*\Theta_2^*} \begin{pmatrix} 1 - \Theta_1^* - \Theta_2^* \\ \mu\Theta_2^* \end{pmatrix}.\tag{63}$$

Noting that Eq. (63) is independent of k , we obtain

$$\begin{pmatrix} \Theta_1^* \\ \Theta_2^* \end{pmatrix} = \begin{pmatrix} \rho_{1,k}^* \\ \rho_{2,k}^* \end{pmatrix} = \frac{1}{\lambda + \mu + 1} \begin{pmatrix} 1 \\ \lambda \end{pmatrix},\tag{64}$$

for any k . The degree distribution does not affect the steady state. A lesson is that the degree distribution influences the population behavior only when there is at least one neighbor-*independent* transition route. It is easy to show that degree distributions are also irrelevant in the voter model (Fig. 8(B)) and cyclic interaction models with more than three states (Sato et al., 2002; Szabó and Sznaider, 2004). In contrast, the rock-scissors-paper game with an additional death rate ($1 \rightarrow 0$) (Tainaka, 2003) is expected to belong to the class analyzed in Sec. 5.

7 Two-population Model

When there are multiple types of distinct populations, they interact without mutating from one to another. As an example, we take a model for malaria spreads (Anderson and May, 1991, Ch. 14). Following the original notation, the meanfield dynamics are represented by

$$\begin{aligned}\dot{y} &= \frac{ab\Omega}{N}(1-y)\psi - \gamma y, \\ \dot{\psi} &= acy(1-\psi) - \mu\psi,\end{aligned}\tag{65}$$

where y and ψ are the proportions of infected humans and mosquitoes, respectively. The size of the human population is denoted by N , and Ω is the size of the female mosquito population; only female mosquitoes infect humans. In addition, a is the bite rate, b and c are infection rates, γ is the recovery rate of the humans, and μ is the death rate of the mosquitoes. Infected humans and infected mosquitoes survive simultaneously if they do. Based on Eq. (65), this occurs when

$$R_0 \equiv \frac{a^2bc\Omega}{N\gamma\mu} > 1.\tag{66}$$

How does this condition change by introducing heterogeneous contact rates? Since neither human-human nor mosquito-mosquito infection is present, the relevant network is bipartite. Two parts represent the human population and the mosquito population. Let us denote the degree distributions of humans and mosquitoes by $\{p_{y,k}\}$ and $\{p_{\psi,k}\}$, respectively. Real data suggest that neither $\{p_{y,k}\}$ nor $\{p_{\psi,k}\}$ is scale-free. However, we treat general degree distributions so that we can infer complex-network consequences of other multi-population contagion processes. The dynamics are given by

$$\begin{aligned}\dot{y}_k &= \frac{ab\Omega}{N}(1 - y_k)k\Theta_\psi - \gamma y_k, \\ \dot{\psi}_k &= ac(1 - \psi_k)k\Theta_y - \mu\psi_k,\end{aligned}\tag{67}$$

where y_k (ψ_k) is the number of infected humans (mosquitoes) with degree k divided by the total number of humans (mosquitoes) with degree k , and

$$\begin{aligned}\Theta_y &\equiv \frac{1}{\langle k \rangle_y} \sum_k k p_{y,k} y_k, & \langle k \rangle_y &\equiv \sum_k k p_{y,k}, \\ \Theta_\psi &\equiv \frac{1}{\langle k \rangle_\psi} \sum_k k p_{\psi,k} \psi_k, & \langle k \rangle_\psi &\equiv \sum_k k p_{\psi,k}.\end{aligned}\tag{68}$$

The steady state is calculated as

$$(y_k^*, \psi_k^*) = \left(\frac{ab\Omega\Theta_\psi^* k}{N\gamma + ab\Omega\Theta_\psi^* k}, \frac{ac\Theta_y^* k}{\mu + ac\Theta_y^* k} \right),\tag{69}$$

which is solved trivially by $(\Theta_y^*, \Theta_\psi^*) = (0, 0)$. To explore nontrivial solutions, let us eliminate Θ_ψ^* from Eqs. (68) and (69) to obtain

$$\Theta_y^* = \frac{1}{\langle k \rangle_y} \sum_k \frac{ab\Omega k^2 p_{y,k} \sum_{k'} \frac{ac\Theta_y^* k'^2 p_{\psi,k'}}{\mu + ac\Theta_y^* k'}}{N\gamma \langle k \rangle_\psi + ab\Omega k p_{y,k} \sum_{k'} \frac{ac\Theta_y^* k'^2 p_{\psi,k'}}{\mu + ac\Theta_y^* k'}}.\tag{70}$$

The RHS of Eq. (70) is less than 1 when $\Theta_y^* = 1$. Then, the recipe in Sec. 2.1 applies; the endemic state results if

$$\frac{\partial}{\partial \Theta_y^*} (\text{RHS of Eq. (70)})|_{\Theta_y^*=0} = \frac{a^2 bc \Omega \langle k^2 \rangle_y \langle k^2 \rangle_\psi}{N \gamma \mu \langle k \rangle_y \langle k \rangle_\psi} > 1,\tag{71}$$

which extends Eq. (66). Equation (71) indicates that divergence of just either $\langle k^2 \rangle_y$ or $\langle k^2 \rangle_\psi$ is sufficient for the epidemic threshold to disappear. Even if both are finite, their combined effect is magnified by multiplication. This is consistent with the result for the bond percolation on bipartite graphs (Meyers et al., 2003; Newman, 2002).

8 Conclusions

We have analyzed various models of infectious diseases on complex networks. We have not exhausted all possible models. However, our systematic categorization of the examples suggests the consequences of other epidemic processes. The critical infection rates largely vanish as the variance of the degree distribution diverges, which extends the results for the contact process. There are two exceptions to this general law. The first is the models of competing pathogens with mutation (Secs. 4.1 and 4.2), for which coexistence of the competing strains requires additional meanfield-type conditions on mutation rates. The second is the class of the rock-scissors-paper game, whose steady states are independent of degree distributions. Generally, what essentially matters seems to be gross arrangements of contagion pathways. If there is at least one transmission route independent of the neighbors' states, the behavior of the model depends on degree distributions in the same manner as the contact process does. The only caveat is the case of competing pathogens that can mutate from one to another.

A last note is on the stability of solutions. For the contact process on complex networks, the coexistence phase is duly stable (Anderson and May, 1991; Olinky and Stone, 2004). Similarly, the stability of the simplest nontrivial phase is assured for multi-state models. However, stability analysis of other phases seems mathematically difficult, which is warranted for future work.

References

- Abdullah, A. S. M., Tomlinson, B., Cockram, C. S., and Thomas, G. N. 2003. Lessons from Severe Acute Respiratory Syndrome outbreak in Hong Kong. *Emerg. Infect. Dis.* **9**(9), 1042–1045.
- Albert, R., Jeong, H., and Barabási, A.-L. 2000. Error and attack tolerance of complex networks. *Nature* **406**, 378–382.
- Albert, R., and Barabási, A.-L. 2002. Statistical mechanics of complex networks. *Rev. Mod. Phys.* **74**, 47–97.
- Anderson, R. M., and May, R. M. 1991. “Infectious diseases of humans,” Oxford University Press, Oxford.
- Andjel, E., and Schinazi, R. 1996. A complete convergence theorem for an epidemic model. *J. Appl. Prob.* **33**, 741–748.
- Barabási, A.-L., and Albert, R. 1999. Emergence of scaling in random networks. *Science* **286**, 509–512.
- Cohen, R., Erez, K., ben-Avraham, D., and Havlin, S. 2000. Resilience of the Internet to random breakdowns. *Phys. Rev. Lett.* **85**, 4626–4628.
- Colgate, S. A., Stanley, E. A., Hyman, J. M., Layne, S. P., Qualls, C. 1989. Risk behavior-based model of the cubic growth of acquired immunodeficiency syndrome in the United States. *Proc. Natl. Acad. Sci. U.S.A.* **86**, 4793–4797.
- Durrett, R., and Neuhauser, C. 1991. Epidemics with recovery in $D = 2$. *Ann. Appl. Prob.* **1**(2), 189–206.
- Frean, M., and Abraham, E. R. 2001. Rock-scissors-paper and the survival of the weakest. *Proc. R. Soc. Lond. B* **268**, 1323–1327.

- Goh, K.-I., Kahng, B., & Kim, D. 2001. Universal behavior of load distribution in scale-free networks. *Phys. Rev. Lett.* **87**, 278701.
- Haraguchi, Y., and Sasaki, A. 2000. The evolution of parasite virulence and transmission rate in a spatially structured population. *J. Theor. Biol.* **203**, 85–96.
- Hopbauer, J., and Sigmund, K. 1998. “Evolutionary games and population dynamics,” Cambridge University Press, Cambridge.
- Joo, J., and Lebowitz, J. L. 2004. Pair approximation of the stochastic susceptible-infected-recovered-susceptible epidemic model on the hypercubic lattice. *Phys. Rev. E* **70**, 036114.
- Kobayashi, M., Sato, K., and Konno, N. 2001. Phase diagrams and correlation inequalities for epidemic models. *Trans. Materials Res. Soc. Jpn.* **26(1)**, 365–368.
- Konno, N., Schinazi, R. B., and Tanemura, H. 2004. Coexistence results for a spatial stochastic epidemic model. *Markov Processes Relat. Fields* **10**, 367–376.
- Krone, S. M. 1999. The two-stage contact process. *Ann. Appl. Prob.* **9(2)**, 331–351.
- Leo, Y. S. *et al.* 2003. Severe Acute Respiratory Syndrome – Singapore, 2003. *MMWR* **52(18)**, 405–411.
- Liggett, T. M. 1985. “Interacting Particle Systems,” Springer, New York.
- Liljeros, F. *et al.* 2001. The web of human sexual contacts. *Nature* **411**, 907–908.
- Liu, J., Tang, Y., and Yang, Z. R. 2004a. The spread of disease with birth and death on networks. *J. Stat. Mech.* P08008.
- Liu, J., Wu, J., and Yang, Z. R. 2004b. The spread of infectious disease on complex networks with household-structure. *Physica A* **341**, 273–280.
- Marro, J., and Dickman, R. 1999. “Nonequilibrium phase transitions in lattice models,” Cambridge University Press, Cambridge.

- Masuda, N., Konno, N., and Aihara, K. 2004. Transmission of severe acute respiratory syndrome in dynamical small-world networks. *Phys. Rev. E* **69**, 031917.
- Masuda, N., and Konno, N. 2004. Return times of random walk on generalized random graphs. *Phys. Rev. E* **69**, 066113.
- May, R. M., and Lloyd, A. L. 2001. Infection dynamics on scale-free networks. *Phys. Rev. E* **64**, 066112.
- Meyers, L. A., Newman, M. E. J., Martin, M., and Schrag, S. 2003. Applying network theory to epidemics: control measures for *Mycoplasma pneumoniae* outbreaks. *Emerg. Infect. Dis.* **9**(2), 204–210.
- Moreno, Y., Pastor-Satorras, R., and Vespignani, A. 2002. Epidemic outbreaks in complex heterogeneous networks. *Eur. Phys. J. B* **26**, 521–529.
- Newman, M. E. J. 2002. Spread of epidemic disease on networks. *Phys. Rev. E* **66**, 016128.
- Newman, M. E. J. 2003. The structure and function of complex networks. *SIAM Rev.* **45**, 167–256.
- Olinsky, R., and Stone, L. 2004. Unexpected epidemic thresholds in heterogeneous networks: the role of disease transmission. *Phys. Rev. E* **70**, 030902(R).
- Pastor-Satorras, R., and Vespignani, A. 2001a. Epidemic spreading in scale-free networks. *Phys. Rev. Lett.* **86**, 3200–3203.
- Pastor-Satorras, R., and Vespignani, A. 2001b. Epidemic dynamics and endemic states in complex networks. *Phys. Rev. E* **63**, 066117.
- Satō, K., Matsuda, H., and Sasaki, A. 1994. Pathogen invasion and host extinction in lattice structured populations. *J. Math. Biol.* **32**, 251–268.
- Sato, K., and Konno, N. 1995. Successional dynamical models on the 2-dimensional lattice space. *J. Phys. Soc. Jpn.* **64**(6), 1866–1869.

- Sato, K., Konno, N., and Yamaguchi, T. 1997. Paper-scissors-stone game on trees. *Memoirs of Muroran Institute of Technology* **47**, 109–114.
- Sato, K., Yoshida, N., and Konno, N. 2002. Parity law for population dynamics of N -species with cyclic advantage competitions. *Appl. Math. Comput.* **126**, 255–270.
- Schinazi, R. B. 1997. Predator-prey and host-parasite spatial stochastic models. *Ann. Appl. Prob.* **7**(1), 1–9.
- Schinazi, R. B. 1999. On the spread of drug-resistant diseases. *J. Stat. Phys.* **97**(1/2), 409–417.
- Schinazi, R. B. 2000. Horizontal versus vertical transmission of parasites in a stochastic spatial model. *Math. Biosci.* **168**, 1–8.
- Schinazi, R. B. 2001a. Balance between selection and mutation in a spatial stochastic model. *Markov Processes Relat. Fields* **7**, 595–602.
- Schinazi, R. B. 2001b. On the importance of risky behavior in the transmission of sexually transmitted diseases. *Math. Biosci.* **173**, 25–33.
- Schinazi, R. B. 2002. On the role of social clusters in the transmission of infectious diseases. *Theor. Pop. Biol.* **61**, 163–169.
- Schinazi, R. B. 2003. On the role of reinfection in the transmission of infectious diseases. *J. Theor. Biol.* **225**, 59–63.
- Schneeberger, A. *et al.* 2004. Scale-free networks and sexually transmitted diseases. *Sexually Transmitted Diseases* **31**(6), 380–387.
- Szabó, G., and Sznajder, G. A. 2004. Phase transition and selection in a four-species cyclic predator-prey model. *Phys. Rev. E* **69**, 031911.
- Tainaka, K. 1994. Vortices and strings in a model ecosystem. *Phys. Rev. E* **50**, 3401–3409.

Tainaka, K. 2003. Perturbation expansion and optimized death rate in a lattice ecosystem. *Ecol. Modelling* **163**, 73–85.

van den Berg, J., Grimmett, G. R., and Schinazi, R. B. 1998. Dependent random graphs and spatial epidemics. *Ann. Appl. Prob.* **8(2)**, 317–336.

Figure captions

Figure 1: The transition rule of the contact process. The solid line represents transition independent of states of neighbors, whereas the dashed line represents the neighbor-dependent transition. The values indicate the transmission rates, where n_i ($i = 1$ here) is the number of vertices in state i in the neighborhood.

Figure 2: The rule of the SIRS model.

Figure 3: The rules of (A) the two-stage contact process and (B) the tuberculosis model.

Figure 4: The rules of the models with competing pathogens. (A) example 1, (B) example 2, and (C) example 3.

Figure 5: Numerically obtained stationary densities of (A) state 1 and (B) state 2 for example 1 (Fig. 4(A)). The scale-free networks with $\gamma = 2.5$ (thickest solid lines), $\gamma = 3.0$ (moderate solid lines), $\gamma = 4.0$ (thinnest solid lines), and the random graph (dotted lines) are used. See the text for other parameter values.

Figure 6: The rule of the model with two different types of neighbor-dependent contagions.

Figure 7: (A) The curve $f_1 = 0$ (solid lines), (B) the curves $f_1 = 0$ (solid lines) and $f_2 = 0$ (dashed lines) when $r > 0$, and (C) when $r = 0$.

Figure 8: The rules of (A) the rock-scissors-paper game and (B) the voter model.

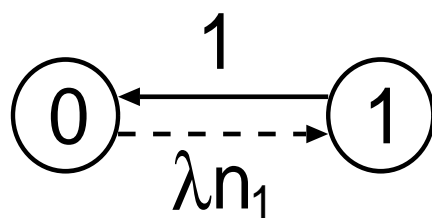


Fig. 1.

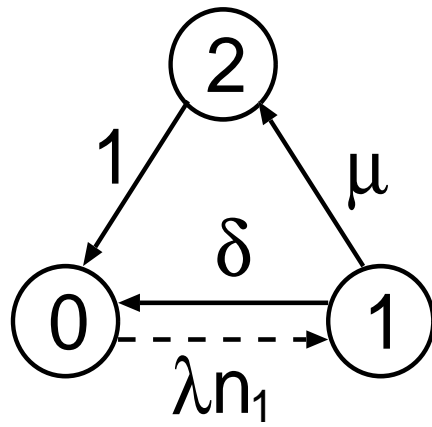


Fig. 2.

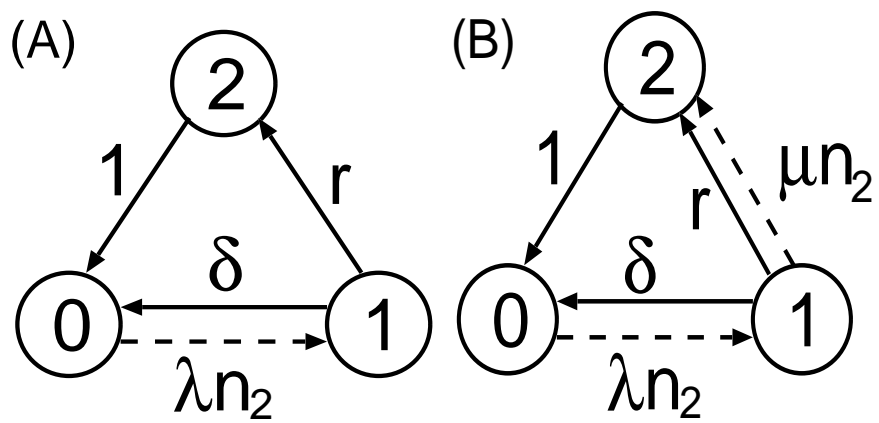


Fig. 3.

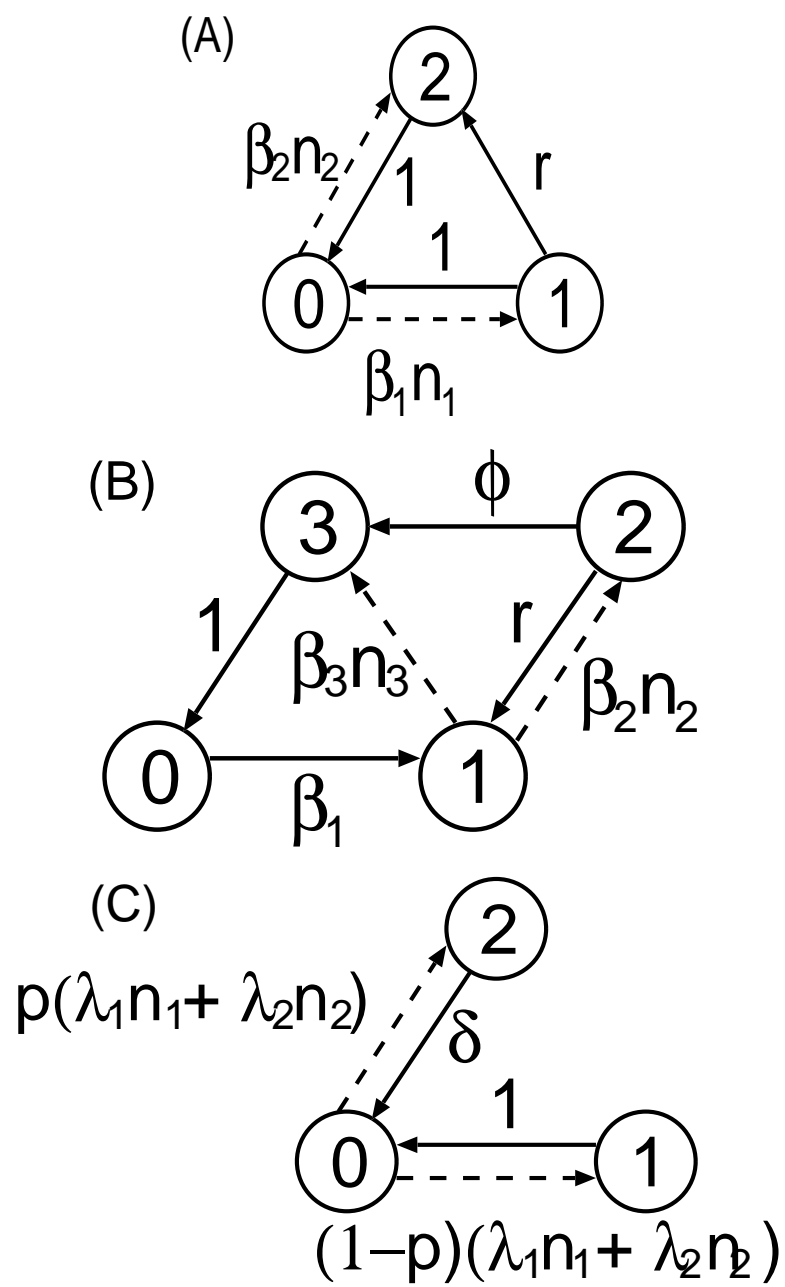


Fig. 4.

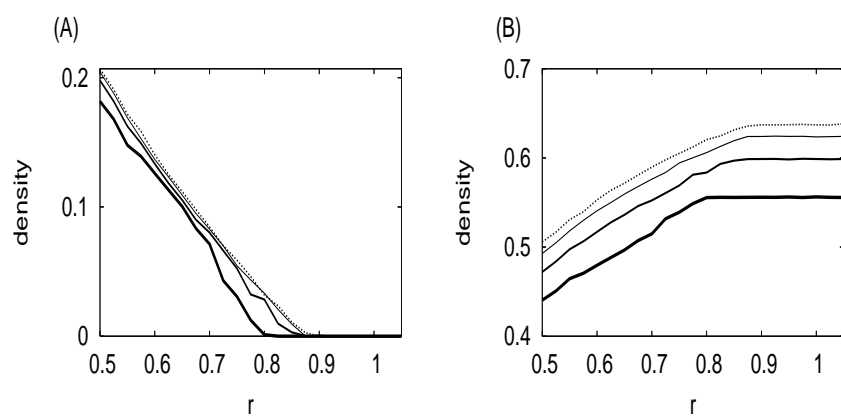


Fig. 5.

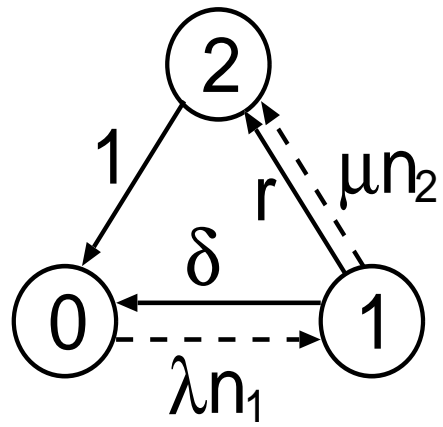


Fig. 6.

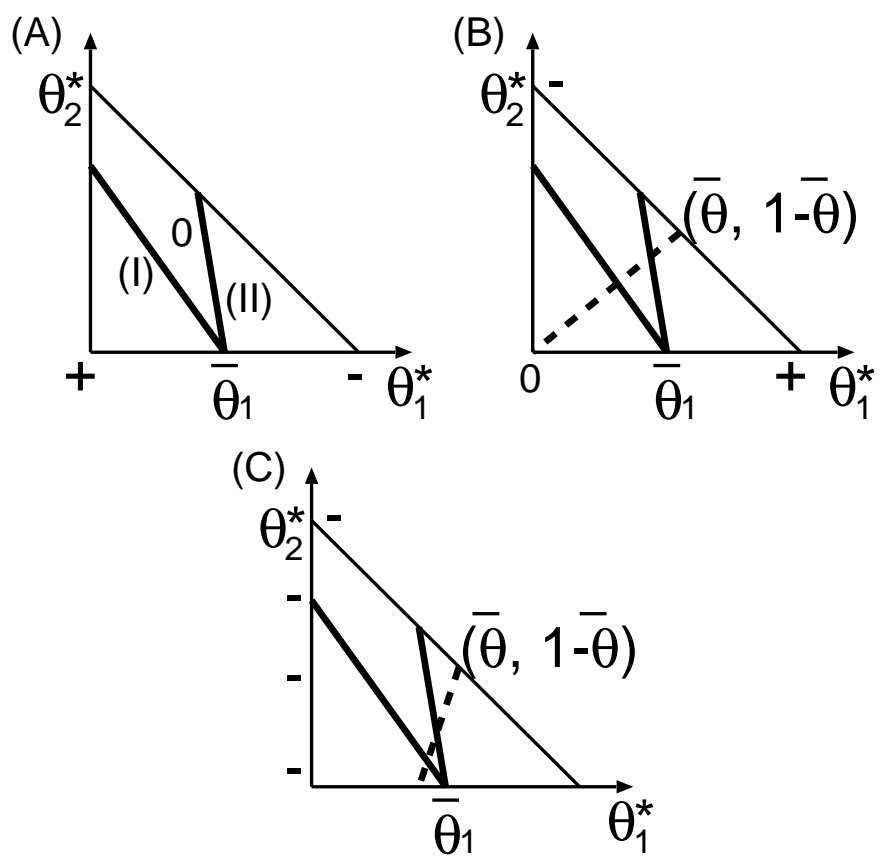


Fig. 7.

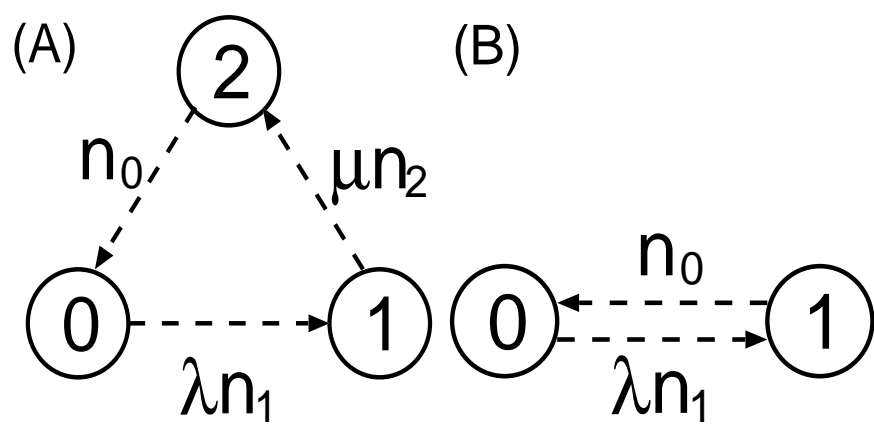


Fig. 8.